Innovative Food Science and Emerging Technologies 48 (2018) 274–286

Contents lists available at ScienceDirect

Innovative Food Science and Emerging Technologies

journal homepage: www.elsevier.com/locate/ifset

Computational evaluation of food carrier designs to improve heating uniformity in microwave assisted thermal pasteurization

Deepali Jain[a], Juming Tang[a,*], Frank Liu[a], Zhongwei Tang[a], Patrick D. Pedrow[b]

[a] Biological Systems Engineering Department, Washington State University, Pullman, WA 99164, USA
[b] School of Electrical Engineering and Computer Science, Washington State University, Pullman, WA 99164, USA

ARTICLE INFO

Keywords:
Microwave heating
Heating uniformity
Pasteurization
Computer simulation

ABSTRACT

Microwave assisted thermal pasteurization system (MAPS) is a novel food safety technology that employs carriers made from stainless steel to move pre-packaged foods inside 915 MHz single mode microwave cavities to eliminate bacterial and viral pathogens. This paper studied the performance of metal carriers for 16 oz and 10 oz food packages in the MAPS. A simulation model built with Quick-wave software was developed to analyze the electromagnetic field distribution inside a MAP system as affected by the presence of the metal food carriers. Computer simulations were validated using a mashed potato model food processed in a pilot scale MAP system; heating patterns of the samples were detected by a chemical-marker based computer vision method. Results showed that different designs of the food carriers could be used to modify electric field distribution to obtain relatively uniform heating patterns within the microwave cavities. Simulation results also illustrated that magnetron frequency variations between 900 MHz and 920 MHz do not affect the heating patterns of food packages processed using carriers containing metal parts. The results demonstrated that the MAPS with moving metal carriers has stable and predictable heating patterns.

Industrial relevance: Microwave transparent materials such as plastics have been used to make transport carriers for food packages in microwave assisted thermal sterilization (MATS) (Tang, 2015). However, polymers may have a short life in the high-temperature processing conditions and thus may not be desirable in an industrial setting. The simulations and experiments conducted in this work showed that the novel concept of metal tray carrier is an effective mechanism for transporting pre-packaged foods in microwave heating systems. The validated computer simulation model presented in this work will be a time efficient, economical and convenient tool to evaluate tray carrier designs for efficient and uniform microwave heating in MAPS.

1. Introduction

Pasteurization is a food preservation technique that involves applications of temperatures in the range of 70–95 °C for a certain length of time to inactivate viral pathogens and vegetative bacterial cells (Peng et al., 2017; Bhunia et al., 2016). Microwave assisted thermal pasteurization system (MAPS) is a novel technology developed at Washington State University for pasteurization of pre-packaged food products. The MAPS technology is based on simultaneous heating of food by microwaves and hot water (Resurreccion et al., 2013). Fig. 1 provides a schematic of a pilot scale MAPS. It has four sections, i.e. preheating, microwave heating, holding and cooling sections, each section is filled with circulating water at a set temperature. MAPS microwave cavities are designed to operate in single mode at 915 MHz which ensure predictable and stable heating patterns as explained in detail by Tang (2015). The combination of hot water and microwave heating results in shorter processing time than conventional surface heating methods, and hence better quality of food products (Tang, 2015). Non-uniform microwave heating may be a major challenge in large scale industrial systems where high microwave power is used for the processing. It is possible that the food at the hot spot locations may be overcooked to acheived the required thermal lethality at the cold spots. Therefore, for the commercialization of the technology, small temperature differences between hot and cold spots are highly desirable to improve food quality.

Single mode cavity design in combination of circulating water in the MAPS system provided flexibility for placing and moving different types of materials, including metals, inside the microwave cavities (Tang & Liu, 2017). Specially designed tray carriers made up of rectangular thin metal sheets, and cylindrical shape Polyetherimide (*Ultem*

* Corresponding author at: Department of Biological Systems Engineering, Washington State University, P.O Box 646120, Pullman, WA 99164-6120, USA.
E-mail address: jtang@wsu.edu (J. Tang).

https://doi.org/10.1016/j.ifset.2018.06.015
Received 30 April 2018; Received in revised form 18 June 2018; Accepted 28 June 2018
Available online 02 July 2018
1466-8564/

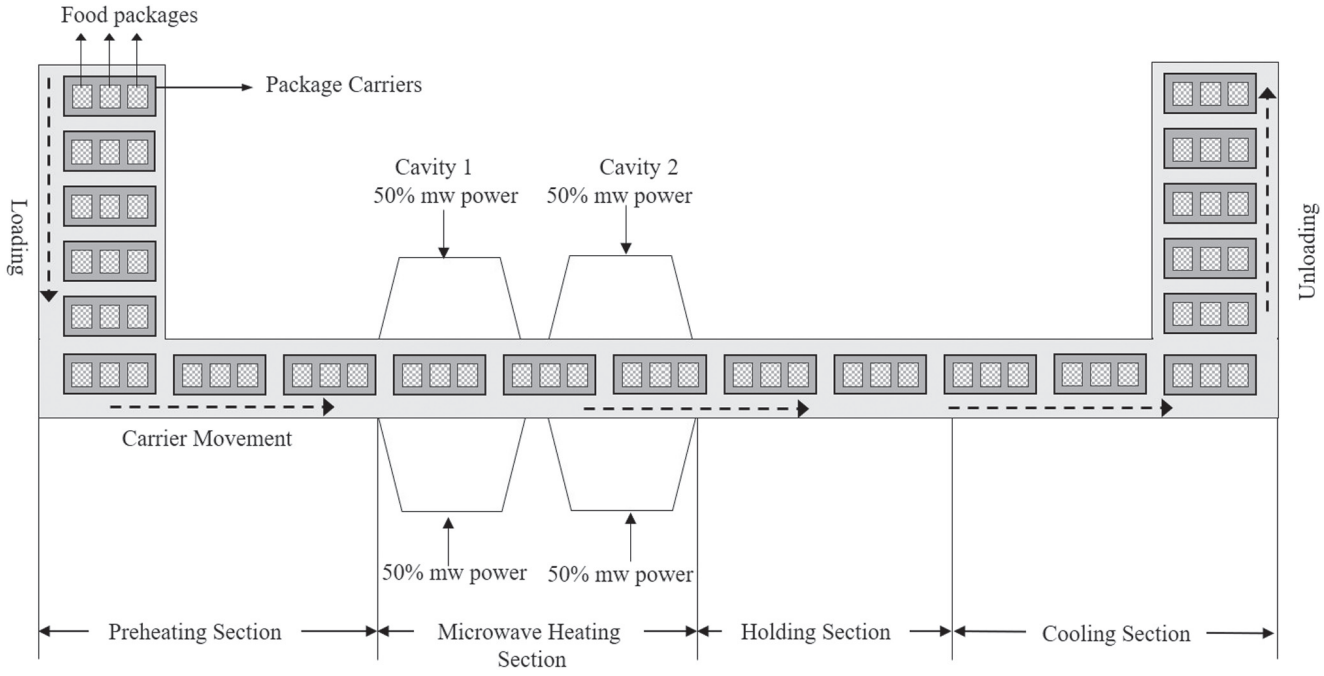

Fig. 1. Schematic diagram for pilot scale microwave assisted thermal pasteurization system consisting of preheating, microwave heating, holding and cooling sections.

TM) parts were used to distribute the electric field more evenly and provide better heating uniformity for 16 oz and 10 oz food packages (Tang & Liu, 2018). The designs of these carriers can be easily configured for different sizes and shapes of the food packages to obtain higher heating uniformity. Use of stainless steel in designing the carriers for food packages also resists corrosion in water immersion system and adds durability. Direct measurement of reflected microwave powers from the cavities indicated that the metal carriers do not adversely affect coupling of microwave energy from the generator. The heating rate at the cold spots in food packages remains similar to that in the packages transported with plastic carriers (Tang & Liu, 2018).

The electromagnetic field distributions inside the microwave cavity is impacted by the presence of food packages and transport carriers leading to variations in heating patterns and temperature profiles. Till now, there are no effective sensors for the accurate measurement of electric field in high permittivity materials such as food. Therefore, a 3-D computer simulation model (CSM) was developed and validated to explore the electric field patterns in pilot scale microwave assisted thermal sterilization system (MATS-CSM) (Resurreccion et al., 2013). The MATS-CSM was used to analyze the electromagnetic field distributions, heating patterns and temperature profiles for foods moving on a polymeric conveyor mesh belt (Resurreccion et al., 2013; Luan et al., 2015; Luan, Tang, Pedrow, Liu, & Tang, 2013; Luan, Wang, Tang, & Jain, 2017). The conveyor belt was microwave transparent; therefore, it was not considered while simulating the MATS system. Design of the MAPS is different from MATS pilot scale system in the manner that food packages are transported throught the microwave cavities. In MAPS, the conveyor mesh belt is replaced by stainless steel carriers. The carriers are loaded with the pre-packaged food and are moved through the cavities on a set of wheels. Different components of the tray carriers interact with the microwave field and aids in directing the microwave energy to the food packages. Movement of objects that can distort the microwave field distributions within the cavities also affect the temperature profiles of the food items. Thus, it is imperative to include the metal transport carriers in the simulation model of the MAPS process. This work was focused to develop and validate a simulation model for MAPS system with newly designed metal carriers. A validated model will be an important tool to design tray carriers for various sizes, shapes and orientations of the food packages to generate more efficient and uniform heating patterns.

In this work, four different types of food carrier designs suitable for 16 oz and 10 oz food packages were studied using computer simulations. Electric field distributions and heating patterns of the food packages were analyzed computationally. For the experimental validation, fructose based chemical marker in the mashed potatoes was used as described in Jain, Wang, Liu, Tang, and Bohnet (2017). The chemical marker technique is based on the browning reaction of reducing sugars in a model food and has been used effectively to study heating patterns in microwave assisted thermal processing (Pandit, Tang, Liu, & Mikhaylenko, 2007; Luan et al., 2013, 2015; Zhang et al., 2015; Resurreccion et al., 2013, 2015).

2. Materials and methods

2.1. Computer simulation procedure

2.1.1. Microwave assisted thermal pasteurization (MAPS): physical system

As illustrated in Fig. 1, the pilot scale MAPS consists of four sections, i.e., preheating, microwave heating, holding and cooling. Each section contains circulating water at different temperature, e.g., preheating at 61 °C, microwave heating, and holding at 75–95 °C and cooling at 25 °C. Microwave heating section consists of two connected rectangular cavities which are connected to a generator by a standard waveguide WR975, through which only TE10 mode is supported. Vacuum sealed food packages are secured onto the tray carriers with the help of metal clips. The carriers packed with food items are placed into the MAPS in the loading area, and are moved into the pre-hating section. After preheating for a certain time, tray carriers are transported to the microwave heating section followed by the holding section. The carriers are then moved to the cooling section, and taken out from the unloading zone. The residence time of the food inside each section is controlled by speed of the moving food carrier.

2.1.2. Simulation software

In this study, the computer simulation model was built in Quickwave 3D (QW-3D, QWED, Poland) version 7.5, that uses finite

difference time domain method to solve Maxwell's equations in three dimensional MAPS microwave cavities. QW-3D editor was used to create the geometry, mesh generation and specification of the simulation parameters (e.g., frequency, power) of the microwave heating section of MAPS. After the geometry was built, the QW-simulator with basic heat transfer module (BHM) was used for the calculation and analysis of electromagnetic and heat transfer parameters. An add-in module of QW3D for moving metallic parts was employed to simulate the translational movement of tray carriers.

2.1.3. Finite difference time-domain (FD-TD) governing equations

Physics of electromagnetic wave propagation is described by set of Maxwell's equations, which can be written in integral form as (Balanis, 2005)

$$\oint_c \vec{E} \cdot \vec{dl} = -\frac{d}{dt} \int\int_s \vec{B} \cdot \vec{ds} \tag{1}$$

$$\oint_c \vec{H} \cdot \vec{dl} = \frac{d}{dt} \int\int_s \vec{D} \cdot \vec{ds} + \int\int_s (\vec{J_i} + \vec{J_c}) \cdot \vec{ds} \tag{2}$$

$$\oint\!\!\oint_s \vec{D} \cdot \vec{ds} = Q^e \tag{3}$$

$$\oint\!\!\oint_s \vec{B} \cdot \vec{ds} = 0 \tag{4}$$

where $\vec{E}$ is the electric field, $\vec{H}$ is the magnetic field, $\vec{D}$ is the electric flux density, $\vec{B}$ is the magnetic flux density. Q^e is the electric charge enclosed by surface S. C is a contour path surrounding the surface S. J_i and J_c are source current density and conduction current density, respectively. Flux densities are defined as

$$\vec{D} = \varepsilon \vec{E} \tag{5}$$

$$\vec{B} = \mu \vec{H} \tag{6}$$

where ε and μ are permittivity and permeability respectively. The set of equations was solved by quickwave software using conformal FDTD technique which is explained in detail by Taflove and Hagness (2005).

2.1.4. Initial and boundary conditions

- In validation tests, the following conditions were used: food trays were conditioned for 30 min of Preheating in MAPS, that allowed the food to reach uniform temperature of 61 °C before the food entered the microwave cavity. Temperature of the circulating hot water in the heating and holding sections of MAPS was held constant at 93 °C by continuous flow of the water. Therefore, in the simulation model for the microwave heating section, the initial temperature of the food was set to be 61 °C, circulating hot water temperature was set at 93 °C. Perfect electric conductor (PEC) boundary conditions were applied to the walls of the microwave heating section as recommended in previous simulation models of MATS system (Luan, Tang, Pedrow, Liu, & Tang, 2016; Chen, Tang, & Liu, 2008).
- The food, circulating water in cavity and Polyetherimide (*Ultem* ™) elements in the tray carriers were defined as dielectric materials. Dielectric and thermal properties of these materials were saved in an external file. QW-BHM automatically reads the file and modifies media parameters in the FDTD cells filled with different media and calculates the temperature evolution. Metal parts of the food carrier were set as perfect electric conductor and adiabatic boundary conditions were applied between PEC and dielectric materials. Since, polymer packaging of the food items was microwave transparent, it was not considered in the simulations.
- For the tests, 8.7 kW total power was applied. The power was assumed to be equally divided among the two cavities and power for each cavity was evenly distributed to two ports (Fig. 1). Electromagnetic dissipated power is related to electric field intensity by following equation (Dibben, 2001):

$$P = 2\pi \quad f\varepsilon_0\varepsilon_r'' \ |E|^2 \tag{7}$$

where f is frequency Hz, ε'' is loss factor, ε_0 is permittivity of air (8.85×10^{-12} F/m) and $|E|$ is electric field magnitude (V/m).
- Only solid and semi-solid food were considered where dominant heat transport mode within the food was conduction following the conduction heat transfer equation (Dibben, 2001):

$$\bigtriangledown^2 T - \frac{\rho C_p}{k}\frac{\partial T}{\partial t} = 0 \tag{8}$$

where ρ is density (kg/m^3), C_p is specific heat (kJ/kg-K) and k is thermal conductivity of food (W/m-K).
- At the food and water boundary, heat flux (q) was governed by convective heat transfer (Bergman & Incropera, 2011),

$$q = h(T - T_s) \tag{9}$$

where h is convective heat transfer coefficient (W/m^2-K), T is food temperature in °C, and T_s is circulating water temperature which was taken as 93 °C. Prior to microwave heating simulations, heat transfer coefficient calculations were performed. Experiments were conducted in MAPS to record the temperature profile history at the cold spot when microwave power was switched off. The capacitance lumped method was used to approximate the value of heat transfer coefficient as described in Bergman and Incropera (2011). Convective heat transfer coefficient (h) between hot circulating water and food packages was set at 190 W/m^2 K.

2.1.5. Dielectric and thermal properties measurement

Dielectric properties of mashed potato model food in the range of 300–3000 MHz was measured using Hewlett-Packard 8752C network analyzer (Palo Alto, CA 94304). The measurements were carried out at temperatures of 22, 30, 40, 50, 60, 70, 80, 90, and 100 °C using the procedures reported in Zhang et al. (2015, 2014) and Auksornsri, Tang, Tang, Lin, and Songsermpong (2018). Mashed potato sample was filled in a cylindrical test cell and temperature of the sample was controlled by circulating oil to the gap between two walls of the test cell from an oil bath. All measurements were conducted in triplicate. Double needle probe KD2 (Decagon Devices Inc, Pullman, WA) was used to measure the thermal conductivity, diffusivity, specific heat of the samples in the temperature range 25–100 °C. A Dual needle (SH-1), 30 mm long, 1.28 mm diameter probe with 6 mm spacing between needles was used.

2.2. Food package carrier designs

16 oz and 10 oz food packages made up of rigid multi-layered polymeric trays with the following structure: PP/regrind/tie/EVOH/tie/regrind/PP (Bhunia et al., 2016) were used to process the samples. Fig. 2 shows the design of the tray carriers for 16 oz [160 (x) × 125 (y) × 25 (z) mm] and 10 oz [90 (x) × 135 (y) × 25 (z) mm] food packages. For each tray size, two designs of the transport carrier were analyzed. The side part of all the carriers was same and made up of Polyetherimide (*Ultem* ™) and rectangular metal plates of specific thicknesses as shown in Figs. 2–5. *Ultem* ™ is a high heat resistance, high mechanical strength and high electric strength material (Jiao, Tang, & Wang, 2014). *Ultem* ™ was also used in a microwave assisted thermal sterilization (MATS) system to alter the electric field distribution within the cavity (Chen et al., 2008). In the MATS system, rectangular slabs of *Ultem* ™ were attached to the cavity walls which helped in controlling the heating patterns (Resurreccion et al., 2013). Similar rectangular slabs of *Ultem* ™ was used in the pasteurization system (MAPS). However, instead of fixing the *Ultem* ™ to the cavity wall, it was attached to the carriers which moved through the cavities. For the food holding part of the carriers, two designs were studied to understand how they scatter and re-distribute the electric field inside

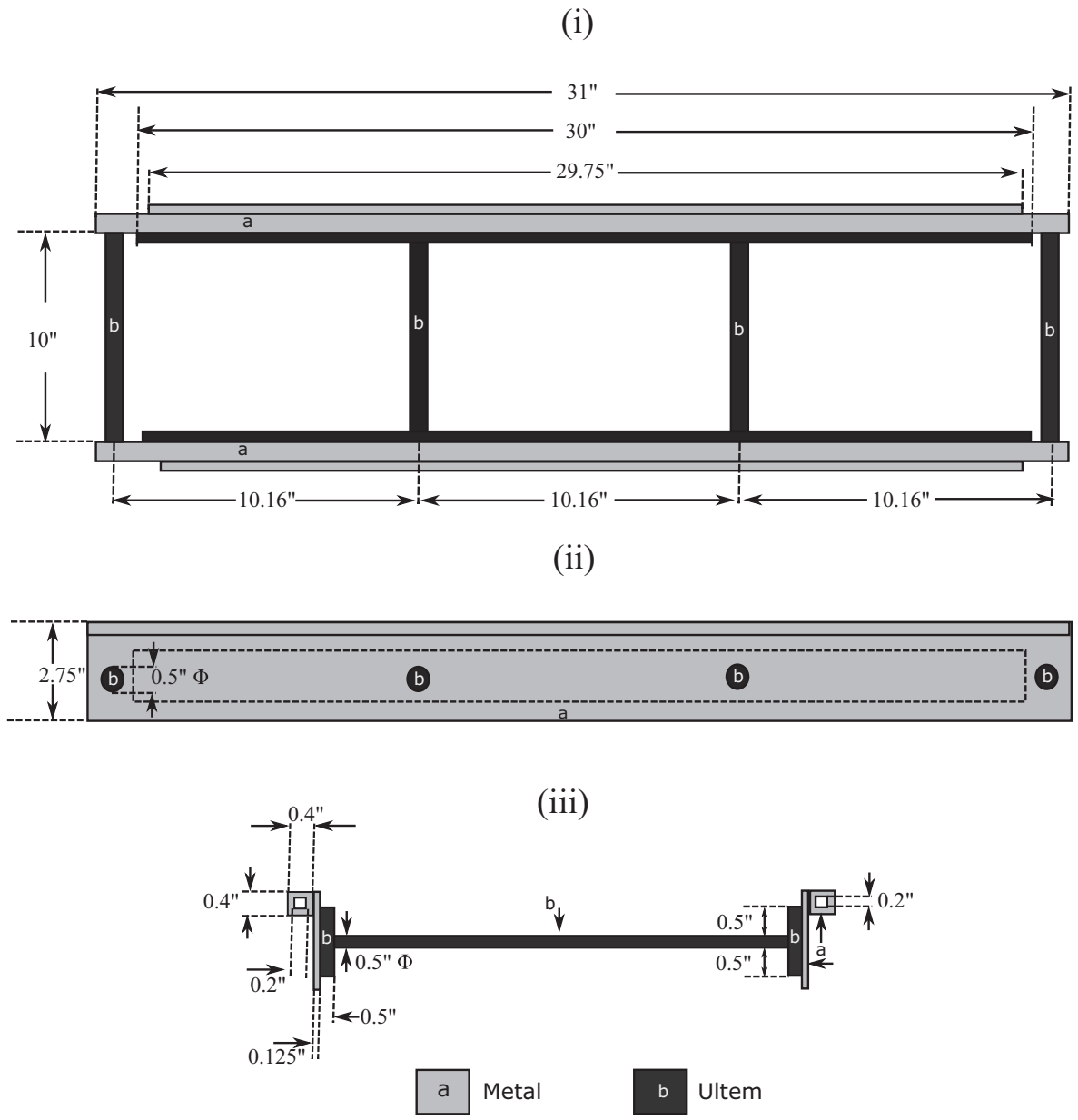

Fig. 2. Tray carrier for 16 oz trays consisting of cylindrical *Ultem* ™ bars in the middle portion (16 A). i) Top view, ii) front view, and iii) side view.

the food package. 1) evenly spaced cylindrical *Ultem* ™ rods were added on the carriers as shown in Figs. 2 and 4. Tray carriers for 16 and 10 oz food packages were fixed with four and seven cylindrical rods, respectively. A plastic mesh with suitable sized pockets for 16 and 10 oz packages was used to secure the food packages in place. This design is referred as 16 A (Fig. 2) and 10 A (Fig. 4) tray carriers for 16 and 10 oz food packages, respectively. 2) A stainless steel frame along the edges of the food packages was employed in the second design (Figs. 3 and 5). The food packages were attached to the carriers using a clip. The metal frame used in the system had perforations to allow the flow of circulating hot water. This design is referred as 16 B (Fig. 3) and 10 B (Fig. 5) tray carriers for 16 and 10 oz food packages, respectively. 16 A or 16 B carriers could carry 3 packages at a time while 10 A or 10 B could carry 6 packages at once.

2.3. Electric field distribution and heating pattern analysis

Fig. 6 shows a 3-D computer model of the microwave heating section of MAPS built using Quickwave software. Computer simulations were performed to study the electric field distribution and heating patterns of food in the two different designs of 16 oz tray carriers (16 A and 16 B; Figs. 2 and 3) and 10 oz tray carriers (10 A and 10 B; Figs. 4 and 5). The electric field patterns in the following cases were analyzed: (1) unloaded cavity, (2) the carrier without food packages in the center of the cavity and, (3) the tray carrier with food in the center of the cavity. In the operation of the MAPS, the food packages moved at the speed of 14.8 mm/s in the x-y plane. For the entire length of the two microwave cavities, the residence time for a package to move through the two microwave heating cavities was 1.7 min. The continuous translational movement of the food packages over 1.7 min was incorporated in the simulation model using a built-in mechanism along a step-wise linear trajectory in the x-y plane, which requires a definition of heating time per simulated time step. The choice of number of discrete time steps and heating time (Δt) at each step is very critical for the convergence and efficient use of the computation resources. Too large Δt may cause computation errors and too small will increase the computation time. Therefore, a heating time sensitivity tests were performed for 8, 16 and 32 steps for the trays to travel two microwave

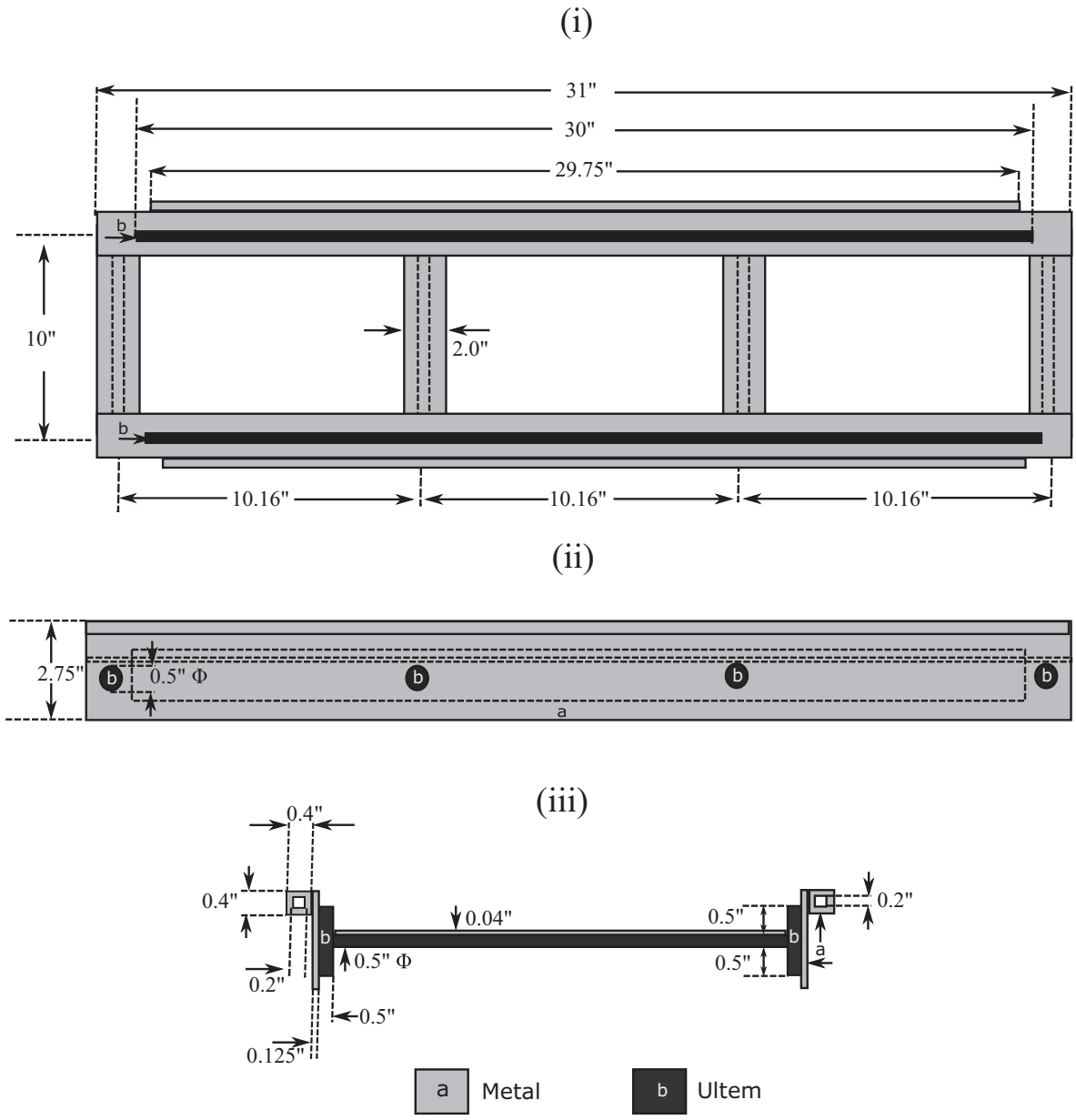

Fig. 3. Tray carrier for 16 oz trays consisting of metal frame (16 B) in the middle portion. i) Top view, ii) front view, and iii) side view.

cavities, as, explained by Resurreccion et al. (2013). It was observed that there were no significant differences in the heating patterns and temperature values obtained using 16 and 32 time steps. Thus, 16-time steps with each step having heating of 6.5 s was used to simulate the movement of the tray carrier. A non-uniform mesh was generated with maximum cell size of 4 mm × 4 mm × 18 mm in the air and 4 mm × 4 mm × 1 mm in water and food according to the 10 points per wavelength rule (Resurreccion et al., 2013). Simulations were performed on a HP Z800 workstation with a dual processor of X5680, 3.33 GHz and a memory of 96 GB. It took 1 h and 30 min to complete computer simulation for one moving position and 24 h to simulate a 16 steps run.

2.4. Validation experiment procedure

Fructose browning in mashed potato model food was used as chemical marker for the validation of the simulated heating pattern as described by Jain et al. (2017). Model food samples were prepared by adding 4% dried potato flakes and 1% gellan gel in water at 90 °C. The mixture was kept at 90 °C and stirred continuously. Heating was stopped when a homogeneous solution was obtained. When temperature of the mixture dropped down to 70 °C, 0.4% liquid titanium dioxide and 1.5% fructose were added. Solution was cooled further to 65 °C, and 0.1% sodium hydroxide (to obtain initial pH 11 in the model food) and 0.3% calcium chloride was added and mixed for 1 min. The solution was then poured into the trays and was allowed to set for 1–2 h in a refrigerator. The food samples were then vacuum packed, and loaded in the food carrier.

A MAPS process schedule was selected to achieve a lethality for a 6 log reduction of psychrotrophic non-proteolytic Clostridium botulinum type E ($P_{90\ °C}$ = 10 min) at cold spot in the model food. The process is aimed to obtain shelf life of up to six weeks at 5 °C in low acid foods (Peng et al., 2017). Model food samples packaged in 16 oz or 10 oz food trays were placed on the carriers and loaded in the preheating section with circulating water at 61 °C in the pilot scale MAP system (Fig. 1). After 30 min, the carriers were moved to the microwave heating section at a speed of 14.8 mm/s for 1.7 min of heating in the two microwave cavities. Temperature of circulating water in the microwave cavity was

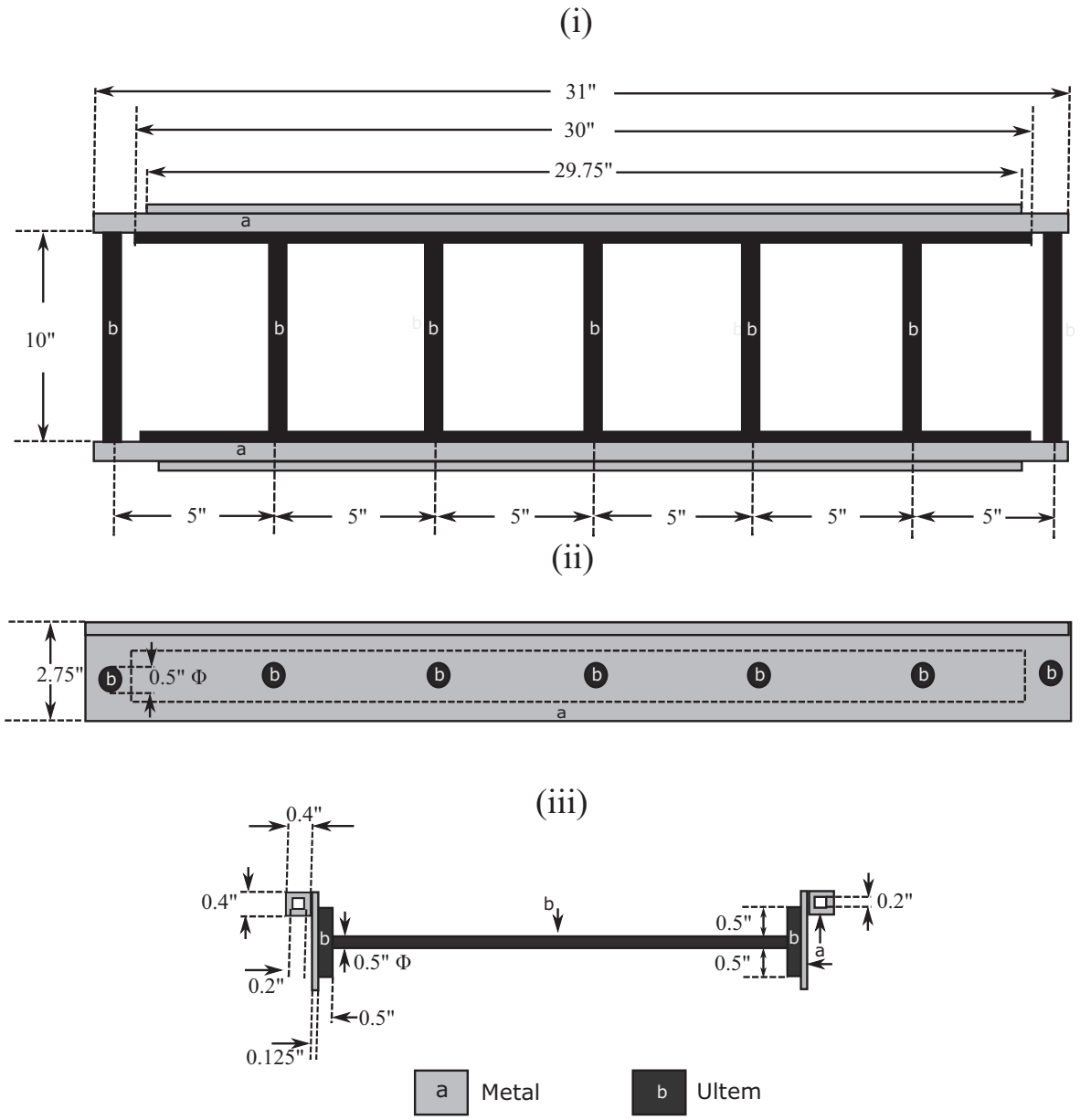

Fig. 4. Tray carrier for 10 oz trays consisting of cylindrical *Ultem* ™ bars in the middle portion (10 A). i) Top view, ii) front view, and iii) side view.

set at 93 °C. Samples were then kept in holding section for 280 s and then they were moved to cooling section at 25 °C. After cooling down food packages were unloaded from the system.

To determine the heating patterns, the processed food was cut from the middle layer in x-y plane and pictures were captured using the camera set up described in Pandit, Tang, Liu, and Pitts (2007). The images were then analyzed using the computer vision system (CVS) technique discussed in Pandit, Tang, Liu, and Mikhaylenko (2007). The analysis used a CS6 Photoshop (Adobe system, Inc., San Jose, CA) and an IMAQ vision builder software (National Instrument Product, Austin, TX). The CVS method maps the heating intensity of the samples based on the change in color of the samples due to formation of brown pigments in the model food during thermal processing. The areas which received the most heat treatment were converted to red color, medium heat treatments area were changed to green color and least heated areas were represented by the blue color.

For further validation, mobile metallic temperature sensors (TMI-Orion, Castelnau-le-Lez, France) were imbedded in model foods processed under the same conditions as above to record the temperature differences between hot and cold spots in the food trays. Prior to the tests, the mobile sensors were glued on a rubber cushion inside the food tray such that the tip was fixed at the predetermined hot and cold spot locations and did not move during the processing. Temperature sensors were placed perpendicular to the electric field component as suggested by Luan et al. (2013) to minimize the interference of the microwaves with the sensors and ensure accurate reading. After fixing the sensors, mashed potato model food was filled in the trays and was processed in the MAPS as described above. The cumulative lethality (P) was calculated from the recorded temperature data using following equation (Holdsworth, 1997):

$$P = \int_0^t 10^{(T-T_{ref})/z} dt \tag{10}$$

T is temperature of food in °C, T_{ref} is 90 °C and z value is 9.84 °C.

2.5. Effect of frequency on heating pattern

The heating pattern of the food in a microwave assisted thermal

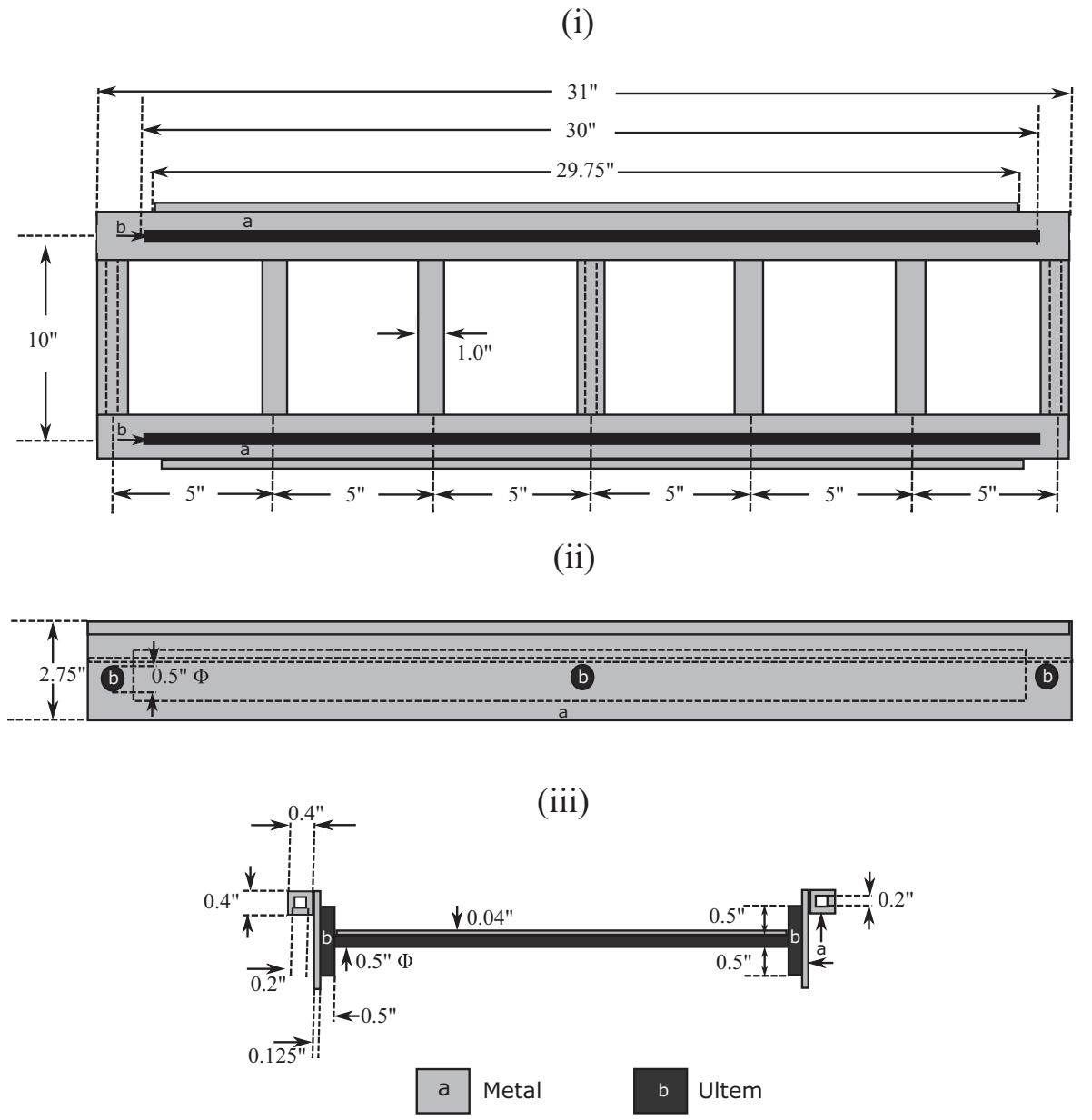

Fig. 5. Tray carrier for 10 oz trays consisting of metal frame in the middle portion (10 B). i) Top view, ii) front view, and iii) side view.

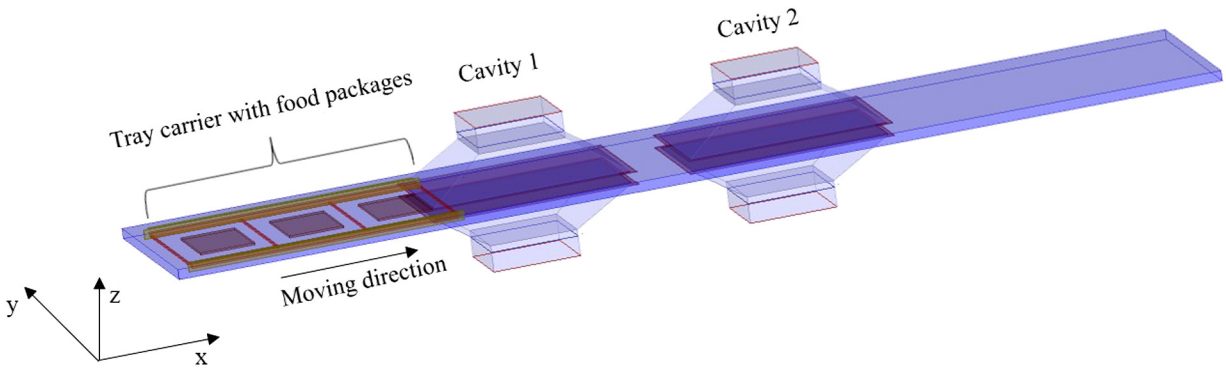

Fig. 6. Computer simulation model for pilot scale microwave assisted thermal pasteurization system consisting of microwave heating section and the tray carrier with food packages.

Table 1
Dielectric properties at 915 MHz, specific heat and conductivity of mashed potato model food measured at temperature range 25 °C–100 °C.

T (°C)	ε_r'	ε_r''	c (kJ/kg-°C)	K (W/m-°C)
25	72.8 ± 2.0	15.5 ± 0.9	2.51 ± 0.32	0.44 ± 0.04
30	74.2 ± 2.1	16.6 ± 1.2	2.60 ± 0.39	0.47 ± 0.06
40	73.5 ± 2.4	18.1 ± 0.8	2.84 ± 0.21	0.53 ± 0.02
50	72.2 ± 2.1	19.5 ± 0.9	2.96 ± 0.10	0.56 ± 0.03
60	70.5 ± 1.7	21.4 ± 1.0	3.09 ± 0.10	0.59 ± 0.05
70	68.9 ± 1.4	23.5 ± 0.5	3.20 ± 0.06	0.60 ± 0.03
80	67.1 ± 0.5	25.5 ± 0.1	3.51 ± 0.14	0.63 ± 0.09
90	65.2 ± 0.2	27.8 ± 0.3	3.24 ± 0.12	0.66 ± 0.09
100	62.3 ± 1.0	29.3 ± 0.2	3.81 ± 0.44	0.69 ± 0.12

process is determined by the resonant modes within the microwave cavity. Each resonating mode has a corresponding resonance frequency (Sadiku, 2010). In case of multi-mode cavities, small shift in frequency may result in a different mode type and unpredictable heating patterns (Luan et al., 2017). MAPS uses single mode cavities designed to operate at 915 MHz. Operating frequency may be affected by factors such as magnetron brand, design, age and power settings. The Federal Communications Commission (FCC) of the United States designated 915 ± 13 MHz for medical, scientific and, industrial (MSI) uses other than telecommunications. Therefore the simulation model was used to determine the effect of change in frequency on the heating pattern of the food for various designs of the carriers. Frequencies in MAPS were recorded under 4, 8, 12 and 16 kW power settings using the TM-2650 spectrum analyzer (BK Precision, California) as described in Resurreccion et al. (2015). Measurements for each power settings were done in 10 replicates. Simulation cases to determine the heating pattern

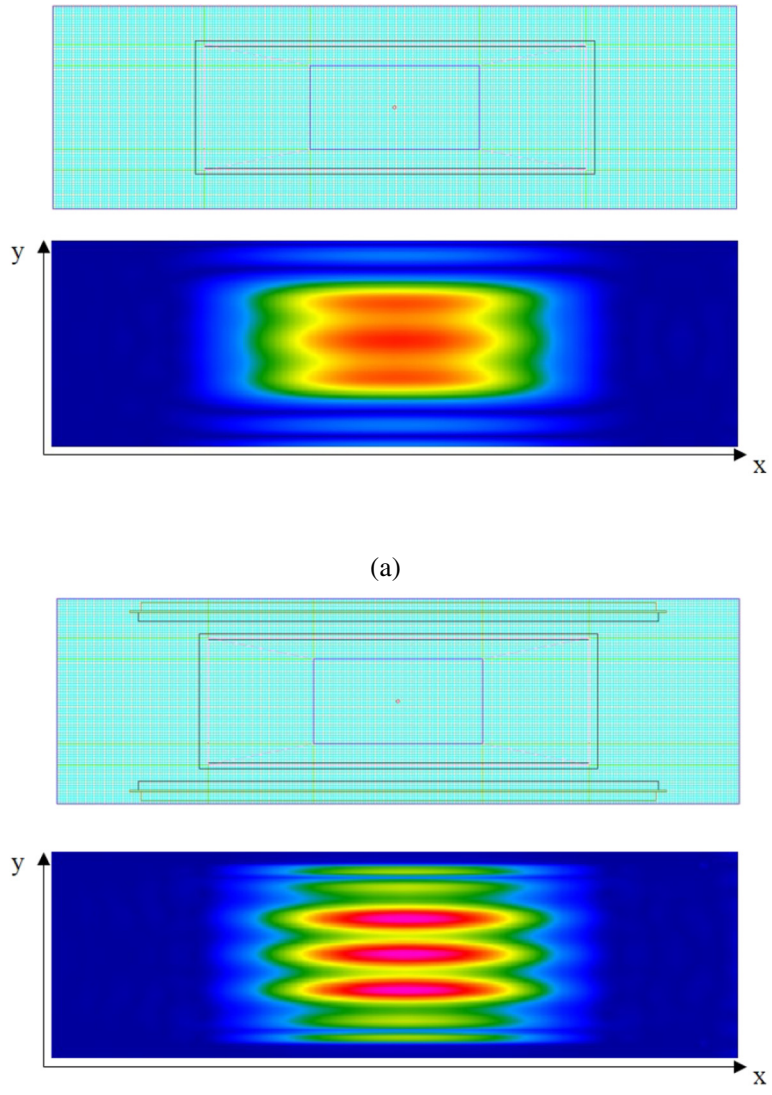

Fig. 7. Total electric field distribution (E) in the central plane of a MAPS cavity. a) Empty. b) In the presence of tray carrier without food packages.

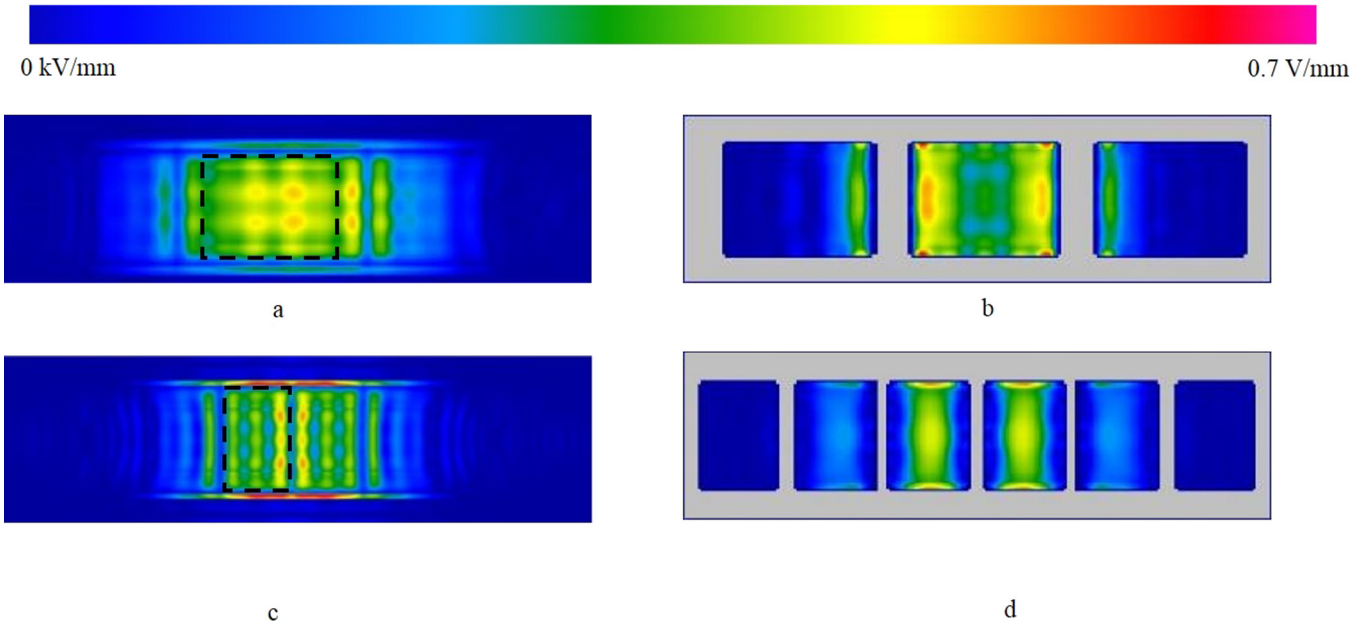

Fig. 8. Electric field distribution inside the cavity when tray carrier with food packages was placed in the center. (a) 16 A, (b) 16 B, (c) 10 A, and (d) 10 B; black dashed lines represent locations of 16 oz food package and 10 oz food packages in sub-figures (a) and (c), respectively.

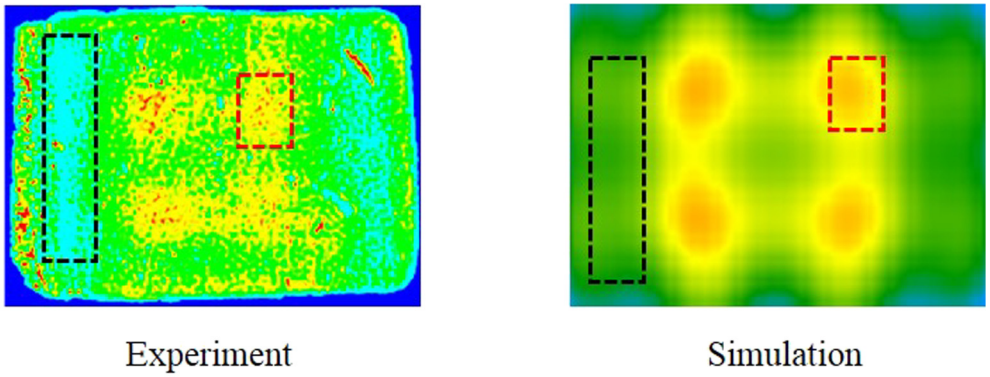

Fig. 9. Heating patterns in 16 oz food packages loaded into tray carrier designs. a) 16 A and b) 16 B; left image is experimental heating patterns obtained by chemical marker in model food; right image is simulation results. Areas in red and black boxes represent hot and cold spots respectively. (For interpretation of the references to color in this figure legend, the reader is referred to the web version of this article.)

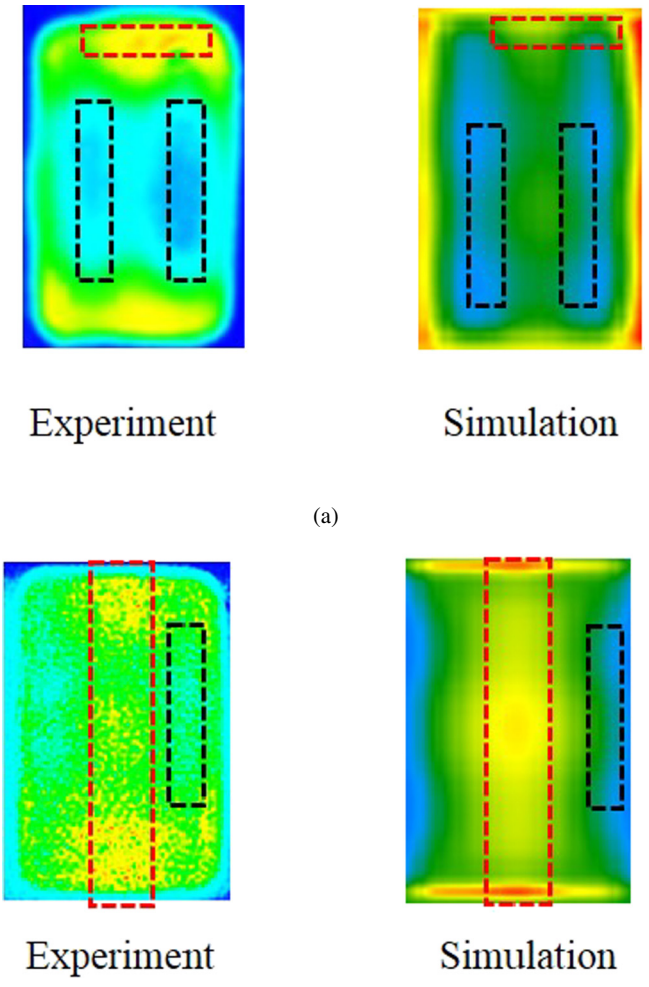

Fig. 10. Heating patterns in 10 oz food packages loaded into tray carrier designs. a) 10 A and b) 10 B; left image is experimental heating patterns obtained by chemical marker in model food; right image is simulation results. Areas in red and black boxes represent hot and cold spots respectively. (For interpretation of the references to color in this figure legend, the reader is referred to the web version of this article.)

Table 2
Operating frequencies of MAPS generator for various power settings.

Transmitted microwave power (kW)	Peak operating frequency (MHz)
4	904.4 ± 1.0
8	906.3 ± 0.5
12	908.7 ± 0.4
16	910.2 ± 0.2

were performed in the range of 900–920 MHz which is in the range of MSI allocation.

3. Results and discussion

3.1. Properties of dielectric materials

Dielectric and thermal properties of mashed potato model food at 915 MHz in the temperature range 20 °C to 100 °C are listed in Table 1. The dielectric constant of the model food decreased as the temperature increased, whereas, loss factor, specific heat, and conductivity increased with increasing temperature. The property data obtained in this work showed similar trend and range as reported in the literature for food materials (Guan, Cheng, Wang, & Tang, 2004; Pu, Song, Song, & Wang, 2017; Rao, Rizvi, Datta, & Ahmed, 2014; Spieß et al., 2001). Free water dispersion, bound water dispersion, and ionic conduction governs the dielectric properties of a food material (Feng, Tang, & Cavalieri, 2002). The gradual decrease in the dielectric constant with increasing temperature in the model food was likely due to the dispersion of free water molecules (Feng et al., 2002). Ionic conduction is the dominant mechanism for loss factor at frequencies lower than 1 GHz (Guan et al., 2004). Therefore increase in loss factor with increase in temperature was attributed to the increase in conductance of the model food. A sharp change in dielectric properties of foods with change in temperature may lead to thermal runaway heating during microwave processing (Guan et al., 2004). However at 915 MHz, change in the loss factor and dielectric constant for the food was not very drastic, which is an advantage of MAPS in providing relatively uniform heating profiles. For circulating water in the heating section, dielectric constant of 60 and loss factor of 2.37 at 915 MHz and 93 °C were obtained which was in agreement with the previous measurements by Komarov and Tang (2004) and Resurreccion et al. (2015). *Ultem* ™ had dielectric constant of 3.2 and loss factor of 0.003 (Jiao et al., 2014). These property data were used as the inputs in the simulation model to define food, water and *Ultem* ™ as the dielectric materials.

3.2. Influence of food carriers on electromagnetic field distribution in MAPS

Fig. 7 (a) shows total electric field in the central plane of an unloaded microwave cavity with circulating water at 93 °C. A staggered electric field pattern with 3 distinct high intensity field zones in y direction was observed. For the heating uniformity TE20 or TE 30 mode was recommended (Luan et al., 2016). In the MAPS system an unloaded cavity was designed to operate at TE30 mode. Electric field distribution in the cavity in the presence of the tray carrier without food trays is shown in the Fig. 7 (b). The side metal and ultem parts of the carrier did not affect the main operating modes. However, the intensity of the electric field was higher when the tray carrier was present compared to unloaded cavity. It may be possible that the structures made from different materials influenced the microwave scattering and reflection within the cavity leading to higher electric field intensities.

Fig. 8 shows the electric field distribution in the cavity with 16 oz or 10 oz tray carriers with food packages in the center of the cavity. Black dashed lines in Fig. 8a and c represent locations of the 16 oz food package (160 mm × 125 mm) and 10 oz food package (90 mm × 135 mm), respectively. For the 16 A tray, four high intensity zones were observed (Fig. 8a). These zones were equally spaced within the food package and were away from the edges. Within one food package, electric field intensity near the edges of the food package was low compared to middle portion of the food package. Near the *Ultem* ™ rods, high intensity electric fields were observed. *Ultem* ™ bars are dielectric cylinders which scatter and absorb microwaves thus may be responsible for creating a localized high intensity zone in near vicinity. The tray carrier surrounded by perforated metal plate (16 B) resulted in two high power zones at the edges in y direction (Fig. 8b). The electric field in the presence of metal frame was concentrated on the edges instead of at the center. Thus the simulations showed that in this design the edges of the food packages will be intensively heated by hot water as well as microwaves which may lead to severe edge heating.

For the 10 oz tray carriers, with *Ultem* ™ cross rods (10 A), the electric field was concentrated near the edges of the food along y direction (Fig. 8c). 10 oz food packages have smaller x dimensions than 16 oz (90 mm for 10 oz vs. 160 mm for 16 oz package). Therefore, in 10 A tray carrier there were seven *Ultem* ™ rods (Fig. 4) and food packages were closer to the rods compared to the 16 oz food packages in 16 A tray carrier (Fig. 2). The close proximity of food packages to the *Ultem*

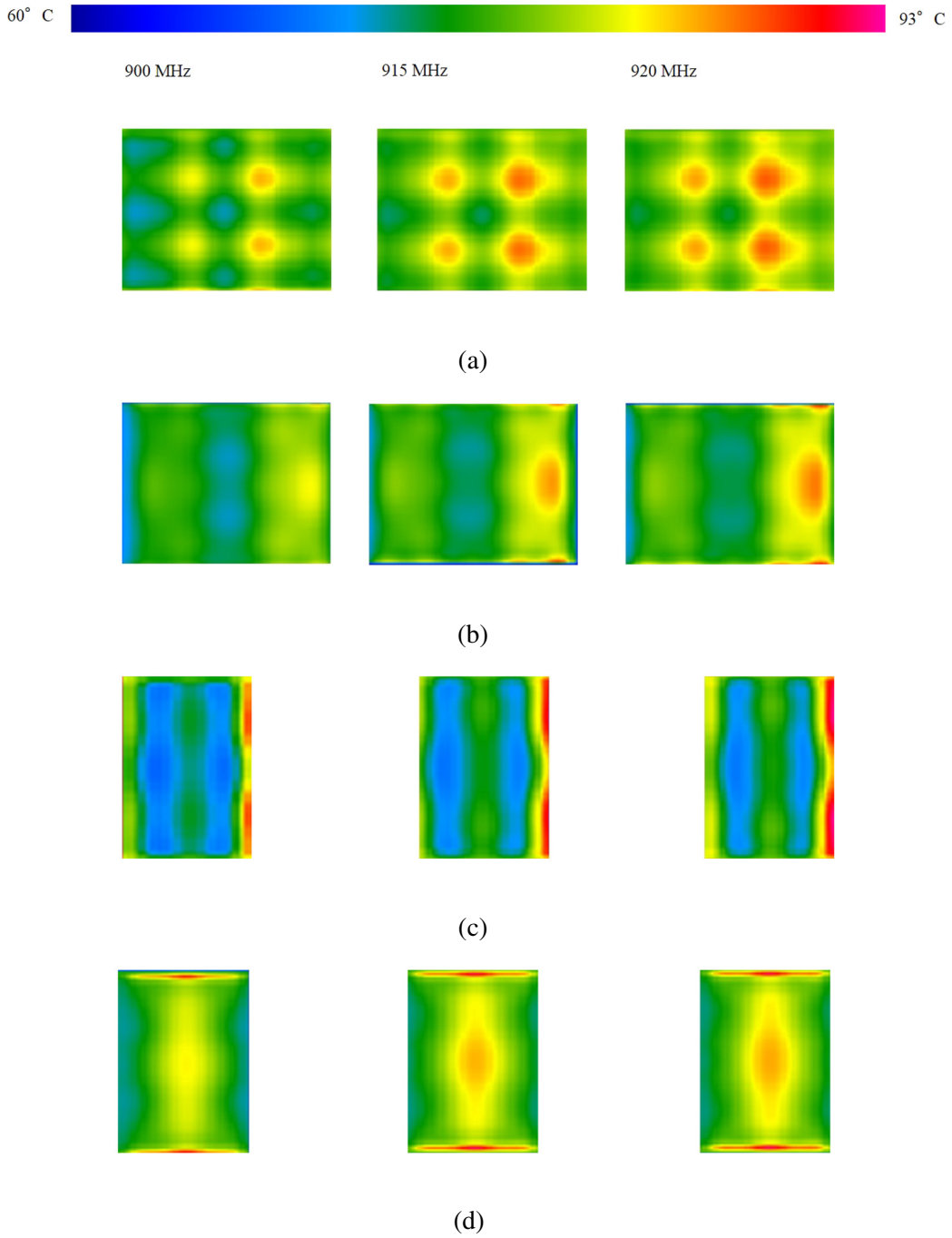

Fig. 11. Heating patterns in the middle layer of food tray for four designs of the carrier at 3 frequency values. (a) 16 A, (b) 16 B, (c) 10 A, and (d) 10 B.

TM rods might be responsible for the high intensity zones near the edges in 10 oz food packages. In the second design of the 10 oz carrier (10 B), the presence of the metal frame surrounding the food led to electric field distribution focused in the center and away from the vertical (y direction) edges of the tray (Fig. 8d). Therefore it was predicted that microwaves will heat the food in the center of the packages placed in the 10 B food carrier. Since in the MAPS, the cavity was filled with the hot water, the edges of the food would be heated by the circulating water. Thus it was anticipated that the design of simultaneously heating by water and microwaves will provide better heating uniformity for 10 oz food packages in 10 B tray carrier.

3.3. Heating patterns using simulations and experiments

For the heating pattern simulations, electromagnetic and heat transfer equations were solved simultaneously for the assigned heating time duration. The simulated heating patterns within the food packages were obtained in the central plane (x-y) immediately after the microwave heating is complete. Experiments were performed using chemical marker method, processed samples were cut in the central layer and were analyzed using computer vision assistant method (Pandit, Tang, Liu, & Mikhaylenko, 2007). Figs. 9 and 10 shows a comparison of experimental and simulated heating patterns. Red zones represent hot spots and blue areas show the cold spots. For both of the designs of 16 and 10 oz tray carriers, simulation results matched very closely with the experimental heating patterns. Chemical marker heating patterns also

validated the electric field distribution obtained in the cavity. High electric field intensity areas correspond to the hot spots, and low intensity areas correspond to cold spots.

For further validation, after determining locations of the hot and cold spots using computer vision system (CVS), temperatures were recorded at hot and cold spot locations of all four designs i.e. 16 A, 16 B, 10 A and 10 B. Temperature difference between hot and cold spot at the exit of second cavity and overall lethality were calculated to indicate the heating uniformity.

In case of the 16 oz tray carrier designs, the temperature difference between cold and hot spots at the exxit of the second microave caviy was 12.1 °C and 15.9 °C for 16 A and 16 B, respectively. 16 B in which food was surrounded by perforated metal frame resulted in higher difference in the cold and hot spot temperatures (15.9 °C). As anticipated from the simulation results, the electric field for this design was concentrated on the edges instead of at the center. Thus edges were heated by hot water as well as microwaves, and the cold spot at the center was heated slowly. Whereas in the case of the 16 A tray carrier, the cold spot location was near the edge which got more hot water heating than the central part, and thus temperature differences between hot and cold spot was 12.1 °C. For the 10 oz tray carrier designs, 10 B was better for heating uniformity compared to 10 A which was anticipated as per simulation results. Experimental temperature profile recording showed that the temperature difference between cold and hot spot was 5.1 °C in 10 A. The difference was reduced to 1.7 °C at the exit of second cavity for 10 B. The difference in lethalities at cold spot and hot spot was 5.3 min in case of the 10 A design. This was reduced to 4.8 min when 10 B was used, showing overall higher uniformity when metal frame was employed.

Temperature difference in 16 oz food packages was higher for both tray carrier designs compared to the 10 oz food packages. Several factors might be responsible for this observation. For example, 16 oz packages were larger, which might lead to slower heat transfer to cold spots. *Ultem* ™ cross bars were responsible for the scattering of the microwave power and distributing it evenly, less number of cross bars in 16 A than 10 A may have resulted in higher temperature differences. Thus it can be concluded that for 16 oz food packages, tray carrier design with *Ultem* ™ bars (16 A) was more appropriate, however even this design led to temperature differences of 10 °C, which was still high due to the larger size of the tray. Study is in progress to optimize the design of the tray carrier for 16 oz food packages to reduce the temperature differences further.

3.4. Effect of frequency on heating pattern

MAPS cavities were designed to resonate at 915 MHz. However in practical applications, it is well known that magnetrons, do not release single frequency (Resurreccion et al., 2015). Microwave frequency of the generators in MAPS during processing were recorded under different power settings of the system. Table 2 shows operating peak frequency of the generator with 4, 8, 12 and 16 kW settings. Peak operating frequencies were lower than 915 MHz in tested power settings but within the range of allocated frequency range by FCC (± 13 MHz). Also the operating frequency was directly proportional to the power setting. In order to cover the lowest and highest possible operating frequency range, simulation cases were performed for 900, 915 and 920 MHz. Fig. 11 shows heating patterns obtained at different frequencies for all four tray carriers. Results demonstrated that the heating pattern is not affected by the frequency shift of the microwave generator in the frequency range of 900–920 MHz for any design of the tray carrier. However product temperature is affected by the change in the peak frequency. As the frequency increased, hot spot areas and the temperature also increased. Similar results were obtained by Resurreccion et al. (2015) for microwave assisted thermal sterilization (MATS) system where food packages were moved on a conveyor belt made from microwave transparent material. The results in this study showed that even in the presence of metal tray carriers, the heating patterns in MAPS were independent of the frequency variation of the generator, however the temperature of hot areas was directly proportional to the frequency.

4. Conclusion

The durability of machinery and the uniformity of heating are of utmost importance in the industrial scale microwave systems. Understanding the electric field pattern inside the MAPS cavities is a non-trivial but vital task for designing efficient tray carriers. A computer simulation model was developed and used as a tool to study various designs of food package carriers in order to improve the heating uniformity in microwave assisted thermal pasteurization system (MAPS). Computer simulations showed that electric field pattern inside the cavity can be modified by varying tray carrier designs. In the case of the 10 oz tray carriers, best results were obtained when a metal frame surrounding the food package was inserted in the tray carrier. The presence of metal plate helped in homogeneous distribution of the microwave power in the center of the tray. However in the case of the 16 oz tray carriers, presence of metal frame concentrated the power on the edges which led to a higher temperature difference in the hot and cold spots. The model developed in this work will be further used to improve the heating uniformity in the bigger size trays as well as in scale up of the system. The simulation model also may incorporate other components of the MAPS, such as waveguide parts, which are necessary in the calculation of S11 parameter to analyze reflection in the system.

Acknowledgments

The authors would like to thank USDA Agricultural and Food Research Initiative 444 (AFRI) CAP grant 2016-68003-23415 to support this study.

References

Auksornsri, T., Tang, J., Tang, Z., Lin, H., & Songsermpong, S. (2018). Dielectric properties of rice model food systems relevant to microwave sterilization process. *Innovative Food Science & Emerging Technologies, 45*, 98–105.

Balanis, C. A. (2005). *Antenna theory analysis and design*. New Jersey: John Wiley & Sons, Inc.

Bergman, T. L., & Incropera, F. P. (2011). *Fundamentals of heat and mass transfer*. John Wiley & Sons.

Bhunia, K., Zhang, H., Liu, F., Rasco, B., Tang, J., & Sablani, S. S. (2016). Morphological changes in multilayer polymeric films induced after microwave-assisted pasteurization. *Innovative Food Science & Emerging Technologies, 38*, 124–130.

Chen, H., Tang, J., & Liu, F. (2008). Simulation model for moving food packages in microwave heating processes using conformal FDTD method. *Journal of Food Engineering, 88*(3), 294–305.

Dibben, D. (2001). *Handbook of microwave technology for food applications*. New York: Marcel Dekker, Inc.

Feng, H., Tang, J., & Cavalieri, R. P. (2002). Dielectric properties of dehydrated apples as affected by moisture and temperature. *Transactions of the ASAE, 45*(1), 129.

Guan, D., Cheng, M., Wang, Y., & Tang, J. (2004). Dielectric properties of mashed potatoes relevant to microwave and radio-frequency pasteurization and sterilization processes. *Food Engineering and Physical Properties, 69*(1).

Holdsworth, S. (1997). *Thermal processing of packaged foods*. London: Chapman & Hall.

Jain, D., Wang, J., Liu, F., Tang, J., & Bohnet, S. (2017). Application of non-enzymatic browning of fructose for heating pattern determination in microwave assisted thermal pasteurization system. *Journal of Food Engineering*, 1–8.

Jiao, Y., Tang, J., & Wang, S. (2014). A new strategy to improve heating uniformity of low moisture foods in radio frequency treatment for pathogen control. *Journal of Food Engineering, 141*, 128–138.

Komarov, V. V., & Tang, J. (2004). Dielectric permittivity and loss factor of tap water at 915 MHz. *Microwave and Optical Technology Letters, 42*(5), 419–420.

Luan, D., Tang, J., Liu, F., Tang, Z., Li, F., Lin, H., & Stewart, B. (2015). Dielectric properties of bentonite water pastes used for stable loads in microwave thermal processing systems. *Journal of Food Engineering, 161*, 40–47.

Luan, D., Tang, J., Pedrow, P. D., Liu, F., & Tang, Z. (2013). Using mobile metallic temperature sensors in continuous microwave assisted sterilization (MATS) systems. *Journal of Food Engineering, 119*(3), 552–560.

Luan, D., Tang, J., Pedrow, P. D., Liu, F., & Tang, Z. (2016). Analysis of electric field distribution within a microwave assisted thermal sterilization (*MATS*) system by

computer simulation. *Journal of Food Engineering, 188*, 87–97.
Luan, D., Wang, Y., Tang, J., & Jain, D. (2017). Frequency distribution in domestic microwave ovens and its influence on heating pattern. *Journal of food science, 82*(2), 429–436.
Pandit, R., Tang, J., Liu, F., & Mikhaylenko, G. (2007). A computer vision method to locate cold spots in foods in microwave sterilization processes. *Pattern Recognition, 40*(12), 3667–3676.
Pandit, R., Tang, J., Liu, F., & Pitts, M. (2007). Development of a novel approach to determine heating pattern using computer vision and chemical marker (M-2) yield. *Journal of Food Engineering, 78*(2), 522–528.
Peng, J., Tang, J., Barrett, D. M., Sablani, S. S., Anderson, N., & Powers, J. R. (2017). Thermal pasteurization of ready-to-eat foods and vegetables: Critical factors for process design and effects on quality. *Critical reviews in food science and nutrition, 57*(14), 2970–2995.
Pu, G., Song, G., Song, C., & Wang, J. (2017). Analysis of thermal effect using coupled hot-air and microwave heating at different position of potato. *Innovative Food Science & Emerging Technologies, 41*, 244–250.
Rao, M. A., Rizvi, S. S., Datta, A. K., & Ahmed, J. (2014). *Engineering properties of foods*. CRC press.
Resurreccion, F., Tang, J., Pedrow, P., Cavalieri, R., Liu, F., & Tang, Z. (2013). Development of a computer simulation model for processing food in a microwave assisted thermal sterilization (MATS) system. *Journal of Food Engineering, 118*(4), 406–416.
Resurreccion, F. P., Luan, D., Tang, J., Liu, F., Tang, Z., Pedrow, P. D., & Cavalieri, R. (2015). Effect of changes in microwave frequency on heating patterns of foods in a microwave assisted thermal sterilization system. *Journal of Food Composition and Analysis, 150*, 99–105.
Sadiku, M. N. (2010). *Elements of electromagnetics*. New York: Oxford University Press.
Spieß, W. E., Walz, E., Nesvadba, P., Morley, M., van Haneghem, I. A., & Salmon, D. R. (2001). Thermal conductivity of food materials at elevated temperatures. *High Temperatures - High Pressures, 33*, 693–697.
Taflove, A., & Hagness, S. C. (2005). *Computational electrodynamics: the finite-difference time-domain method*. Boston: Artech house.
Tang, J. (2015). Unlocking potentials of microwaves for food safety and quality. *Journal of Food Science, 80*(8), E1776–E1793.
Tang, J., & Liu, F. (2017). Microwave sterilization or pasteurization. Google Patents. (US Patent 9,642,385).
Tang, J., & Liu, F. (2018). Microwave sterilization or pasteurization transport carriers and system. Google Patents. (US Patent App. 15/212,655).
Zhang, W., Luan, D., Tang, J., Sablani, S. S., Rasco, B., Lin, H., & Liu, F. (2015). Dielectric properties and other physical properties of low-acyl gellan gel as relevant to microwave assisted pasteurization process. *Journal of Food Engineering, 149*, 195–203.
Zhang, W., Tang, J., Liu, F., Bohnet, S., & Tang, Z. (2014). Chemical marker M2 (4-hydroxy-5-methyl-3(2H)-furanone) formation in egg white gel model for heating pattern determination of microwave-assisted pasteurization processing. *Journal of Food Engineering, 125*, 69–76.